Spin and valence states of iron in Al-bearing silicate glass at high pressures studied by synchrotron Mössbauer and X-ray emission spectroscopy

ZHU MAO[1],*, JUNG-FU LIN[1], JING YANG[1], JUNJIE WU[1,2], HEATHER C. WATSON[3], YUMING XIAO[4], PAUL CHOW[4] AND JIYONG ZHAO[5]

[1]Department of Geological Sciences, Jackson School of Geosciences, The University of Texas at Austin, Austin, Texas 78712, U.S.A.
[2]Beijing National Laboratory for Condensed Matter Physics, and Institute of Physics, Chinese Academy of Sciences, Beijing 100190, China
[3]Department of Earth and Environmental Science, Rensselaer Polytechnic Institute, Troy, New York 12180, U.S.A.
[4]HPCAT, Carnegie Institution of Washington, Advanced Photon Source, Argonne National Laboratory, Argonne, Illinois 60439, U.S.A.
[5]Advanced Photon Source, Argonne National Laboratory, Argonne, Illinois 60439, U.S.A.

ABSTRACT

High-pressure synchrotron Mössbauer (SMS) and X-ray emission (XES) spectroscopic measurements were conducted to investigate the spin and valence states of iron in (Al,Fe)-bearing magnesium silicate glass ($Mg_{0.79}Fe_{0.10}Al_{0.10}Si_{0.96}O_3$) up to 126 GPa and 300 K. By analyzing the Fe $K\beta$ emission spectra using the integrated relative difference (IRD) method, which accounts for the spectral broadening effects, the derived total spin momentum (S) of the iron in the glass shows no observable changes with pressure within the experimental uncertainties. A two-doublet fitting model representing two diverse local iron atomic environments was used to satisfactorily simulate the high-pressure SMS spectra of iron in the glass. The doublet with an averaged quadrupole splitting (QS) value of 1.94($\pm$0.25) mm/s and chemical shift (CS) of 1.02($\pm$0.25) mm/s at ambient conditions was assigned to be high-spin Fe^{2+}, whereas the second doublet with QS = 0.83($\pm$0.25) mm/s and CS = 0.49($\pm$0.25) mm/s was assigned to be high-spin Fe^{3+}. Increasing pressure continuously elevates the QS of Fe^{2+} from ~2 mm/s at ambient pressure to 3.5 mm/s at 126 GPa, while Fe^{3+} only exhibits a slight increase in the QS to 1.34($\pm$0.25) mm/s. Comparing with previous experimental and theoretical studies on the local geometries and hyperfine parameters of silicate glasses and minerals, we conclude that the occurrence of the extremely high QS of Fe^{2+} in our glass above ~40–50 GPa can be associated with the enhanced density and diverse distortions and geometries of the local Fe^{2+} environments. Our combined XES and SMS results show that both Fe^{2+} and Fe^{3+} ions in Al-bearing silicate remain in the high-spin state, rather than undergoing a spin-pairing transition as proposed previously. Assuming that the silicate glass results can be used as an analog for understanding silicate melts, our results here indicate that iron ions likely experience significant changes in the local environments yet remain overall in the high-spin state in silicate melts at the extreme pressure and temperature conditions of the deep mantle.

Keywords: Silicate glass, high pressure, synchrotron Mössbauer spectroscopy, X-ray emission spectroscopy, lower mantle

INTRODUCTION

Physical and chemical properties of rock-forming silicate melts at pressure and temperature (*P-T*) conditions relevant to the Earth's mantle have attracted extensive research interest in the deep-Earth community (Guillot and Sator 2007; Lee 2005, 2011; Ohtani 1985; Poe et al. 1997; Stixrude and Karki 2005; Tonks and Melosh 1993; Wolf and McMillan 1995; Yarger et al. 1995). These properties hold the key to our understanding on the fractionation of the Earth's mantle in the early stage of the terrestrial planetary evolution (Funamori and Sato 2010; Rigden et al. 1984; Stixrude and Karki 2005; Stolper et al. 1981), the model of lunar formation from a giant impact that caused widespread melting (Cameron and Benz 1991; Stevenson 1987), and the formation of the Large Low Shear Velocity Provinces

(ULVPs) beneath the central Pacific and southern Africa above the core-mantle boundary (Wen and Helmberger 1998; Williams and Garnero 1996). The presence of partially melted materials also has the potential to produce chemically distinct reservoirs in the Earth's mantle, because several incompatible elements, including both trace and major elements [e.g., Fe and Pt group elements (PGEs)], preferentially partition into the melt relative to the surrounding solids (Andrault et al. 2012; Corgne et al. 2005; Nomura et al. 2011). It is thus of great interest to deep-Earth geophysicists and geochemists to have a comprehensive knowledge of the behavior of silicate melts and their solid-counterpart glass analogs at relevant *P-T* conditions of planetary interiors.

A recent experimental study reported an abrupt increase in the partition coefficient of Fe between silicate melts and $(Mg,Fe)SiO_3$ perovskite at ~76 GPa (Nomura et al. 2011). The authors explained that this sudden change in the partition coefficient was caused by the high-spin (HS) to low-spin (LS)

transition of Fe in the system, as supported by their synchrotron X-ray emission spectroscopy (XES) measurements in the glass analog. However, such abnormal behavior of the Fe partition coefficient between melts and solids has not been observed in Al-bearing $(Mg,Fe)SiO_3$ perovskite in a later study (Andrault et al. 2012). Furthermore, a very recent high-pressure XES study, together with new Mössbauer results, has also disputed this HS to LS transition explanation (Gu et al. 2012). We note that proper XES spectral references for the HS and LS states were not used in either of these studies, preventing reliable derivations of the total spin momentum (S) associated with the potential spin-pairing transition of iron in the glasses at high pressures (de Groot 2001; Gu et al. 2012; Nomura et al. 2011).

Based on a series of recent experimental and theoretical studies on the spin and valence states of iron-bearing minerals at high pressures (Lin et al. 2013), it is now well understood that applied pressure can induce spin-pairing transitions of Fe^{2+} and Fe^{3+} in the relatively small octahedral sites (B site) in several minerals including ferropericlase, perovskite, and post-perovskite (Badro et al. 2003; Lin et al. 2012; Mao et al. 2010). However, a survey of recent studies on the spin states of Fe^{2+} and Fe^{3+} in the comparatively larger pseudo-dodecahedral site (A site) with 8–12 coordination numbers in silicate perovskite shows that these iron ions likely remain in the HS state even at lower-mantle pressures (Hsu et al. 2011, 2012; Lin et al. 2012); though, an intermediate spin state of Fe^{2+} has also been proposed (McCammon et al. 2008). These observations can be understood in terms of the volume-driven spin transition in which applied pressure further reduces the volume of the local iron site over-coming the spin-pairing energy to stabilize the LS state, while the extremely high-quadrupole values of the A-site Fe^{2+} can be understood in terms of the lattice distortion.

The structural role of Fe in silicate melts and glasses is much more complex than in crystals of the same composition and is currently under debate because of its various oxidation states and local atomic geometries (Mysen and Richet 2005). Particularly, Fe^{3+} can be four- and six-coordinated in silica-rich melts and glasses and has been shown to be in a mixture of four and six coordination in Ca-bearing silica-rich melts (Calas and Petiau 1983; Giuli et al. 2011; Levy et al. 1976; Mysen and Richet 2005; Mysen and Virgo 1989; Mysen et al. 1984, 1985; Wang et al. 1995). The five-coordinated Fe^{3+} has also been observed in hydrous aluminosilicate glass (Wilke et al. 2006). Although Fe^{2+} was proposed to be predominantly in six-coordination (Boon and Fyfe 1972; Fox et al. 1982; Goldman and Berg 1980; Nolet 1980; Virgo and Mysen 1985), recent experimental studies have shown the presence of four- and five-coordinated Fe^{2+} in silicate melts and glasses (Alberto et al. 1996; Bonnin-Mosbah et al. 2001; Giuli et al. 2002, 2011; Jackson et al. 2005; Rossano et al. 1999, 2000; Waychunas et al. 1988). Due to the complex local environments of Fe and limited experimental studies, it remains highly debated as to whether or not iron ions in silicate melts and glasses can undergo a spin transition at lower-mantle pressures (Andrault et al. 2012; Gu et al. 2012; Nomura et al. 2011). Silicate glasses have long thought to be analogs to melts in the deep-Earth mantle due to their similarities in local atomic structures (Akins et al. 2004; Henderson et al. 2006; McMillan 1984; Mysen and Richet 2005). The local structure of the glass

presents the structure of supercooled liquids at the glass transition temperature that is much lower than the melting temperature (Ediger et al. 1996). The information on the spin and valence states of iron in silicate glasses may provide new insights into understanding physical and chemical properties of iron-rich melts in planetary interiors.

In this study, we have investigated the spin and valence states of Fe in an Al-bearing silicate glass using synchrotron XES and Mössbauer spectroscopy (SMS) in a high-pressure diamond-anvil cell (DAC). XES spectra were used to derive the total S of the $3d$ electrons of Fe ions, while SMS results relate hyperfine parameters to the spin and valence states as well as the abundance of Fe ions in the glass at high pressures. Our XES and SMS results are combined with literature data on melts and glasses to decipher the electronic spin and valence states as well as the local electronic environments of Fe in silicate glasses at high pressures.

EXPERIMENTAL METHODS

[57]Fe-enriched Al-bearing silicate glass (>95% enrichment) was synthesized by mixing MgO, Al_2O_3, [57]Fe_2O_3, and SiO_2. All of the oxides were mechanically well mixed and pressed into a small pellet of 2 to 3 mm in diameter and height. The pressed pellet was wrapped in a Pt wire loop and melted in a vertical tube furnace at 1600 °C for one hour in air. Then it was quenched by rapidly removing the sample from the furnace. Electron microprobe and Mössbauer spectroscopic analyses of the sample showed a bulk, homogeneous composition, $Mg_{0.79}Fe_{0.10}Al_{0.10}Si_{0.96}O_3$ with 22% Fe^{2+} and 78% Fe^{3+} of the total iron, while X-ray diffraction (XRD) measurements did not show any obvious crystalline lines.

The (Al,Fe)-bearing silicate glass was polished down to a 15 m disk in thickness, and sample disks of ~50 m in diameter were loaded into symmetric DACs for high-pressure experiments. The sample for SMS experiments was loaded in a sample chamber with a Re gasket and Ne pressure medium, whereas a Be gasket with cBN gasket insert and mineral oil medium was used for XES experiments. Several 10 m ruby spheres were loaded into the sample chambers and used as the pressure calibrant (Mao et al. 1986).

The glass sample has been first examined by the conventional Mössbauer spectroscopy at ambient conditions. High-pressure SMS measurements at ambient temperature were performed at the HPCAT Sector and Sector 3 of the Advanced Photon Source (APS), Argonne National Laboratory (ANL). An incident X-ray beam with an energy of 14.4125 keV and a bandwidth of 2 meV was used to excite the [57]Fe nuclei in the sample. An avalanche photodiode detector (APD) was used to collect the SMS signals with a typical collection time of ~4 to 6 h for each spectrum. The SMS spectra were collected in pressure steps of ~4 to 12 GPa from 1 bar to 126 GPa. High-pressure and room-temperature XES measurements were also performed at the HPCAT Sector of the APS, ANL. An incident X-ray beam with an energy of 11.3 keV and a bandwidth of ~1 eV was used for the experiments. The collection time for each XES spectrum was ~40 min, and 4 to 6 spectra were added together for a given pressure. Enstatite [$(Mg_{0.75}Fe_{0.25})SiO_3$, En25] was used as the HS reference, whereas ferropericlase [$(Mg_{0.75}Fe_{0.25})O$, Fp25] at 90 GPa was used as the LS reference (Mao et al. 2010).

RESULTS

The conventional Mössbauer spectrum can be well described by a two-doublet model with 21(±5)% of Fe^{2+} and 79(±5)% of Fe^{3+}. The SMS spectra show two dominant quantum beats, which shift to faster time decays with increasing pressure (Fig. 1). Above 100 GPa, these beats become less obvious and the spectra are dominated by a single broad decay. In addition, the spectral intensity at slower decay times above 80 ns slightly increases with pressure. The broadening of the SMS spectra may be caused by the deviatory stress and/or modifications of the local electronic structures in the diamond-anvil cell at high pressures. The SMS spectra were analyzed using the CONUSS program (Sturhahn 2000) (Fig. 1). A two-doublet model was used
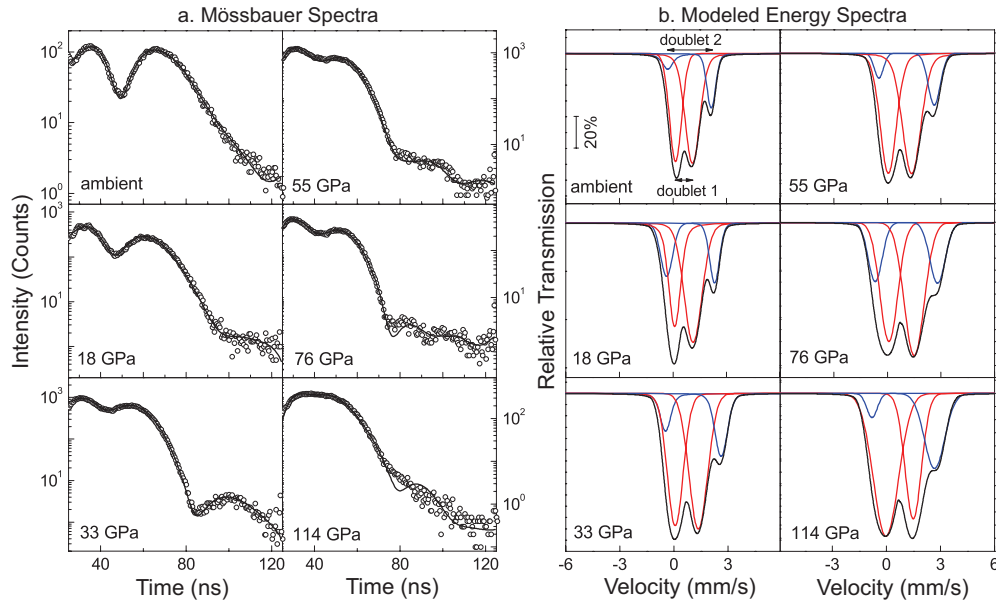
FIGURE 1. Representative Mössbauer spectra of (Al,Fe)-bearing silicate glass ($Mg_{0.79}Fe_{0.10}Al_{0.10}Si_{0.96}O_3$) at high pressures and 300 K. (**a**) Experimentally collected Mössbauer spectra of silicate glass. Circles: measured SMS spectra; black lines: modeled spectra using CONUSS program (Sturhahn 2000); (**b**) Modeled energy spectra of silicate glasses (black line). Red lines: doublet 2 corresponding to Fe^{3+} sites; blue lines: doublet 1 corresponding to Fe^{2+} sites. (Color online.)
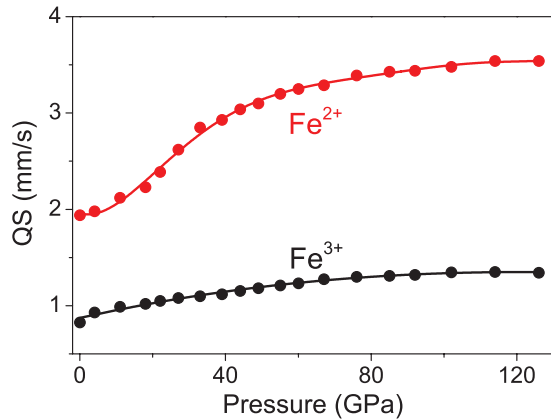

FIGURE 2. Quadrupole splitting (QS) of iron in the silicate glass at high pressures. The lower-QS component is assigned to be Fe^{3+}, while the higher-QS component is Fe^{2+} (see Fig. 6 for details). Solid lines are shown for readers to follow the trend with pressure. (Color online.)

to most satisfactorily simulate the SMS spectra, consistent with results from conventional Mössbauer measurements, although other doublet models were tested and were shown to be not as representative. Since the iron ions in the silicate glass should have diverse distributions of the local geometries with coordination numbers ranging from four to six (Calas and Petiau 1983; Dyar 1985; Giuli et al. 2002, 2011; Jackson et al. 2005; Rossano et al. 1999, 2000; Wilke et al. 2001, 2006), these modeled doublets well represent averaged hyperfine parameters of the iron ions. Because the thermally activated charge transfer between Fe^{2+} and Fe^{3+} valence states is unlikely to occur at ambient temperature

(see further discussion in Discussion section) (Fei et al. 1994; Potapkin et al. 2013), the abundance ratio of these doublets was fixed in our analyses. These analyses show that doublet 1 with 22(±4) % abundance has a QS = 1.94(±0.25) mm/s and CS = 1.02(±0.25) mm/s at ambient conditions. Its QS increases to 3.54(±0.25) mm/s at 126 GPa (Fig. 2). Most importantly, it exhibits a significant increase in the QS between 4 and 55 GPa. Above 55 GPa, its QS shows a much weaker pressure dependence. Doublet 2 has much lower QS [0.83(±0.25) mm/s] and CS [0.49(±0.25) mm/s] values as compared to the doublet 1 at ambient conditions, and shows a smooth increase in the QS to 1.34(±0.25) mm/s at our maximum pressure of 126 GPa (Fig. 2).

At first sight, the raw XES spectra appear to show a subtle, continuous change with pressure up to 80 GPa (Fig. 3). Comparing to the iron-bearing enstatite as the HS reference, the $K\beta$ main peak is slightly widened and the intensity of the $K\beta'$ satellite peak is slightly reduced with pressure. To evaluate the cause for these spectral features, here we have evaluated the XES spectra in two different ways. First, using the integrated absolute difference (IAD) method (Vankó et al. 2006), we have modeled the absolute difference between the sample spectrum and the LS reference (Fig. 3). This difference was later normalized, integrated, and compared with the one from the HS and LS references to derive the S values (Fig. 3). The derived S values obtained in the IAD analyses decrease from 2 to 1.4 with pressure. However, it is well known in spectral analyses that broadening of a spectrum can also lead to the decrease in the intensity of a relatively weaker peak, e.g., in our case here, a weaker satellite peak (de Groot 2001) (Fig. 3). Such broadening effect can be a result of the energy resolution function of the experiments and/ or complex electronic environments at high pressures, and has
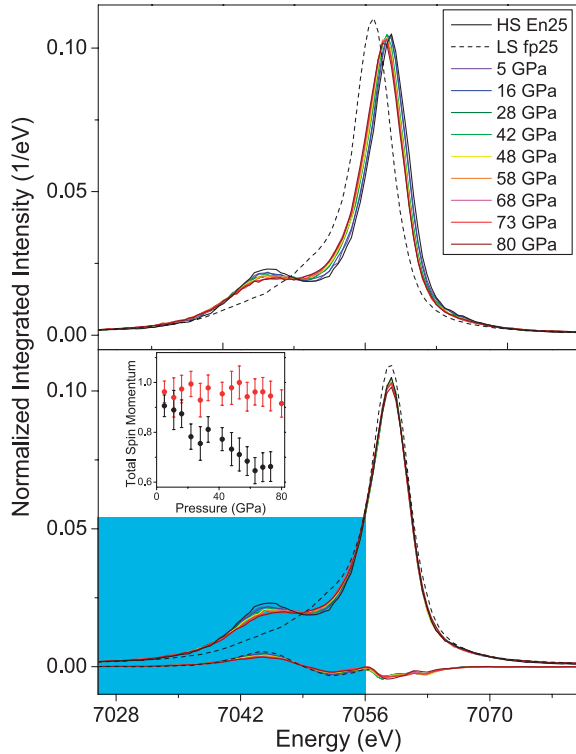
FIGURE 3. X-ray emission Fe K spectra of (Al,Fe)-bearing silicate glass at high pressures and 300 K. (**a**) The XES spectra at various pressures. Fe-bearing enstatite [$(Mg_{0.75}Fe_{0.25})SiO_3$] was used as the high-spin reference (HS En25), while ferropericlase [$(Mg_{0.75}Fe_{0.25})O$] at 90 GPa was used as the low-spin reference (LS Fp25) (Mao et al. 2010); (**b**) XES spectra of silicate glass together with the LS reference (dashed black line) aligned with the HS reference spectrum (solid black line). The difference between the sample spectra (HS spectrum) with the LS reference spectrum is also shown at the bottom. The inserted figure shows the modeled total spin momentum (S) as a function of pressure. The unit of the total spin momentum in the vertical axis is normalized to 1 for the high-spin state of all iron in the glass using their relative abundance ratio derived from the Mössbauer analyses. Red circles represent the derived values using the integrated relative difference (IRD) method. Black circles were calculated using the integrated absolute difference (IAD) method (Vankó et al. 2006). The blue area shows the difference in spectra between the sample spectra (HS spectrum) with the LS reference spectrum, which is used in IRD method. (Color online.)

FIGURE 4. X-ray emission spectra of ferropericlase at high pressures [$(Mg_{0.75}Fe_{0.25})O$, Fp25]. (**a**) XES spectra at selected pressures reported by Lin et al. (2005); (**b**) Derived total spin momentum (S). Red circles: obtained using IRD method; black circles: using the IAD method (Vankó et al. 2006). The fraction of the HS state Fe^{2+} in Fp25 as a function of pressure from previous XRD, RXES, and SMS studies is also shown for comparison (Gavriliuk et al. 2006; Lin et al. 2006, 2010; Mao et al. 2011). (Color online.)

been observed in the previously reported XES spectra (e.g., Lin et al. 2005; de Groot 2001). Specifically, a reduction of the derived satellite intensity in the purely high-spin ferropericlase, which should have a derived $S = 2$, indicates an artifact of the pressure-induced broadening of the emission spectra (e.g., Lin et al. 2005), although such a subtle effect has been neglected in previous analyses (Fig. 4). The broadening effect thus needs to be taken into account in deriving the S values.

Here we report a new XES spectral analytical method to more reliably derive the total spin momentum (Fig. 3). In the analyses, the XES spectra are aligned around the K main peak of the HS reference spectrum and are then integrated using the relative intensity difference of the spectra, herein called integrated relative difference (IRD) method. 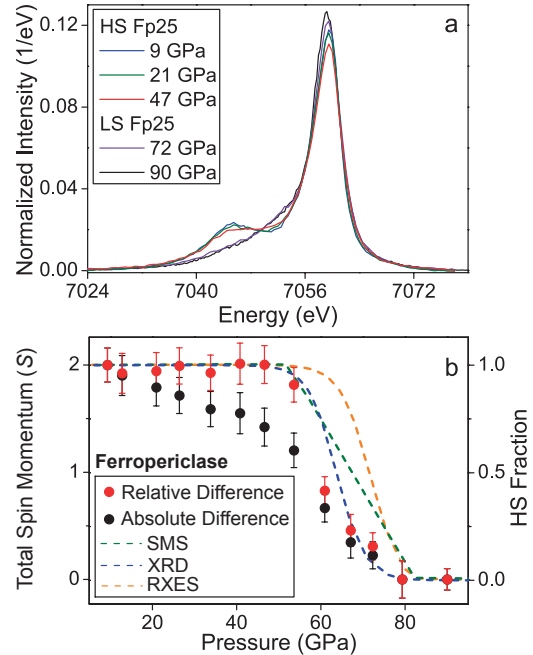Comparison of the aligned spectra with the HS reference clearly shows intensity differences in the whole spectral range; though, these regions have either positive or negative differences. Since the spectral shape can be affected and broadened by applied pressure, this pressure-induced broadening effect produces the region with a negative difference in the satellite $K\beta'$ peak region from the lowest energy to 7049 eV even without a spin transition. The broadening also results in the region with a positive difference from 7049 to 7056 eV. If one was to sum up the differences using the IAD method where all absolute differences were used (Vankó et al. 2006), the integrated intensity would lead to an overestimation of the total spin momentum reduction as a result of the peak broadening alone. To minimize the influence of this broadening effect in the spectral analyses, we have, instead, derived the relative intensity difference between the sample and the HS reference from the lowest energy to the energy at ~7056 eV where the spectral difference is zero near the left shoulder of the K main peak (Fig. 3). This method allows us to directly integrate the difference in the satellite $K\beta'$ peak region that is most sensitive to the $3d$ electronic spin transition while avoiding the broadening effect of the dominant, intense main peak in the XES spectra. The integrated relative differences are then normalized using the difference between the HS and LS reference spectra to derive the total spin momentum. The IRD method we employed here satisfactorily provides results that are consistent with measurements using X-ray diffraction, Mössbauer spectroscopy, and resonant X-ray emission spectroscopy

for ferropericlase [$(Mg_{0.75}Fe_{0.25})O$] (Gavriliuk et al. 2006; Lin et al. 2006, 2010; Mao et al. 2011). On the other hand, derived S values from the IAD method show a broad, continuous decrease with increasing pressure that is not consistent with results from other studies (Gavriliuk et al. 2006; Lin et al. 2006, 2010; Mao et al. 2011) (Figs. 3 and 4). We interpret this continuous decrease as a result of the peak broadening effect at high pressures. The aforementioned comparisons with previous studies further verify the IRD method and justify its use for analyzing the XES spectra of the (Al,Fe)-bearing silicate glass.

DISCUSSION

Total spin momentum of iron in silicate glasses

The electronic spin state of Fe in an Al-free silicate glass has been recently reported to undergo a HS to LS transition at 77 GPa, based on the reduction of the $K\beta'$ satellite peak from high-pressure XES measurements (Nomura et al. 2011); however, the study did not take relevant reference HS and LS spectra into consideration of the spectral analyses. Relevant reference spectra were also lacking in a more recent XES study on two silicate glasses at high pressures (Gu et al. 2012). To derive reliable values of the S and to decipher the spin states of iron ions, we note that it is critical to simultaneously measure reliable HS and LS reference spectra of relevant iron-bearing materials with known spin states for proper data analyses (Figs. 3 and 4). Although the XES spectra are known to be unaffected by the valence states and the coordination numbers between Fe^{2+} and Fe^{3+} (Vankó et al. 2006), the spectral features can be affected by the energy resolution of the incident X-ray source, analyzer, stress states, detector, and applied pressure causing artifacts on the derived S values (de Groot 2001). Additionally, Fe-bearing silicate glasses that are of relevant research interest here only contain dilute amounts of iron ions that have spectral features similar to those in iron-bearing oxides and silicates with minor amounts of Fe^{2+}/Fe^{3+}. However, iron metal and alloys used as references in some previous studies have very distinct spectral features with reduced satellite peaks and narrower band widths of the main peak in the HS state as a result of the strong electron-electron correlations in the system (Lin et al. 2004; Rueff et al. 2001, 2002); these iron alloys belong to strongly correlated systems and cannot be used as reliable references for dilute systems such as the silicate glasses.

Although our collected XES spectra display a slight reduction in the intensity of the $K\beta'$ satellite peak, analyses of the band width of the main peak, together with previous XES data on the HS ferropericlase, suggest that this change is mainly an artifact caused by the broadening of the XES spectra with increasing pressure (Figs. 3 and 4); that is, applied pressure slightly increases the band width of the peaks, which, from the spectral analyses prospect, would certainly reduce the peak intensity of the satellite peak. We note that the XES spectral shape reflects multi-electronic transitions from $3p$ to $1s$ for the main $K\beta$ peak and 3p-3d exchange interactions for the main $K\beta'$ peak (de Groot 2001). The spectral position and shape can thus be affected by applied pressure that modifies the electronic orbital environments, leading to the broadening of the XES spectra at high pressures and at high-stress environments. As shown in our

SMS measurements, the quadrupole splitting of both of Fe^{2+} and Fe^{3+} ions increases with pressure, indicating an increase in the site-to-site atomic distortions of the geometries of the polyhedral surrounding the iron atoms in the glass. The increased distortions of the polyhedral surrounding the iron atoms could result in a wider range of the distribution in the local electric field, leading to the broadening of the XES spectra of glasses. Similar broadening in the XES spectra has also been seen in ferropericlase presented in Lin et al. (2005). To emphasize the importance of correcting the broadening effect when deriving the S value, we have reanalyzed the XES spectra of ferropericlase (Lin et al. 2005) (Fig. 4). Although it is well known that the HS to LS transition of Fe in ferropericlase with 25% iron occurs above 50 GPa, the XES spectra have shown a reduction in the intensity of the $K\beta'$ satellite peak below 50 GPa (Fig. 4). Our analyses here indicate that this is caused by the aforementioned broadening of the XES spectra at high pressures. The S value derived using the IAD method, which does not take this broadening effect into account, decreases from 2 at 1 bar to 1.4 at 47 GPa, although Fe in ferropericlase is observed to be in the HS state at this pressure range in other studies (Fig. 4) (Gavriliuk et al. 2006; Lin et al. 2006, 2010; Mao et al. 2011). Such results with a continuous decrease in the derived S value as function of pressure are inconsistent with recent high-pressure X-ray diffraction (XRD), resonant X-ray emission spectroscopy (RXES), and Mössbauer results (Fig. 4b) (Gavriliuk et al. 2006; Lin et al. 2006, 2010; Mao et al. 2011). After correcting the broadening effect using the IRD method noted above, the derived S value ($S = 2$) remains almost constant between 1 bar and 47 GPa within experimental uncertainties. The S starts to decrease at ~50 GPa when the HS to LS transition of Fe occurs, and drops to 0 at ~80 GPa when the HS to LS transition ends (Fig. 4). The pressure region for the HS to LS transition of Fe in ferropericlase derived from this method is in excellent agreement with that obtained from the previous SMS, RXES, and XRD studies (Gavriliuk et al. 2006; Lin et al. 2006, 2010; Mao et al. 2011), confirming the need to take the broadening effect into account when analyzing the XES spectra.

Based on these analyses, we conclude that the total spin number of our silicate glass does not change with increasing pressure up to 80 GPa after correcting the broadening effect (Fig. 3). That is, both Fe^{2+} and Fe^{3+} ions remain in the HS state at pressures up to 80 GPa (see discussions on Mössbauer results for other details). This conclusion is in distinct contrast to the report by Nomura et al. (2011) but is, to the first order, consistent with the recent study (Gu et al. 2012), although the observed reductions in satellite intensities by Gu et al. (2012) were treated as a partial spin-pairing transition. We note that the composition of the glass sample used by Nomura et al. (2011) was $(Mg_{0.95}Fe_{0.05})SiO_3$, which did not contain any Al, while one of the samples in Gu et al. 2012 ($0.2FeSiO_3–0.05Al_2O_3–0.75MgSiO_3$) and our sample contain some amount of Al. Based on previous experimental and theoretical studies, the presence of Al does not affect the stability of the Fe spin state at high pressures (Catalli et al. 2010, 2011; Hsu et al. 2012). The inconsistency among these studies may be partially explained by different energy resolutions and use of the reference spectra within the experimental conditions, together with the consideration of the broadening effects on the spectra (de Groot 2001; Figs. 3 and 4).
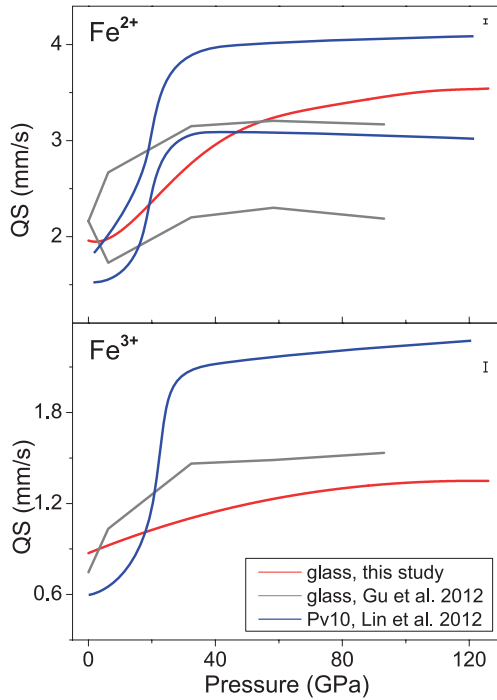
FIGURE 5. Comparison of the quadrupole splitting of (Al,Fe)-bearing silicate glass and a representative silicate perovskite as a function of pressure. Red lines: Al-bearing silicate glass (this study); blue lines: perovskite [$Mg_{0.9}Fe_{0.1}SiO_3$] (Lin et al. 2012); gray lines: $0.2FeSiO_3 0.05Al_2O_3 0.75MgSiO_3$ glass (Gu et al. 2012). The representative error bar of QS is shown at the top right corner of the figure. (Color online.)
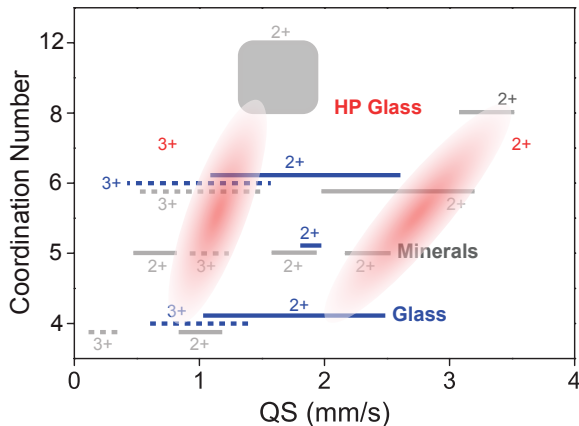

FIGURE 6. Representative quadrupole splitting (QS) values of minerals and silicate glasses as a function of the coordination number (CN) of the iron site at ambient conditions. Our QS results, together with expected CN values of the glass from literature results (Dyar 1985), at high pressures are shown as red areas. Solid lines: QS of Fe^{2+} at ambient conditions; dashed lines: QS of Fe^{3+} at ambient conditions; gray color: representative silicate minerals (Burns 1994; Dyar et al. 2006); gray square: Fe^{2+} in the A site (8 to 12 coordination number) of silicate perovskite (Lin et al. 2012, 2013); blue: representative silicate glasses (Dyar 1985); red area: potential increase in the coordination number of the Fe ion in glass at high pressures (Benmore et al. 2011; Funamori et al. 2004). (Color online.)

Hyperfine parameters of iron in silicate glasses

Analyses of the SMS spectra provide direct information on the hyperfine parameters (QS and CS) of the iron ions, which can be used to refer the spin and valence states of Fe in minerals and glasses (Burns 1994; Dyar 1985; Dyar et al. 2006), because each iron ion with a specific spin and valence state should have distinct characteristics of the relevant hyperfine parameters. Since the local atomic environments of the iron ions in silicate glasses are very diverse, their hyperfine parameters are expected to be broadly distributed when compared to minerals with distinct iron sites (Burns 1994; Dyar 1985; Dyar et al. 2006). The modeled energy spectra from SMS measurements show a distinct broadening with pressure, with a full-width at half maximum increasing from 0.77 mm/s at ambient conditions to 1.87 mm/s at 126 GPa, indicating that applied pressure indeed increases the disorder of the iron ions in the system (Fig. 1). As shown from the analyses of the SMS spectra in the (Al,Fe)-silicate glass, the QS of both modeled doublets increases with pressure (Fig. 2). Comparing our results with previous studies on silicate glasses and minerals at ambient conditions, together with the XES analyses, the hyperfine parameters of the two doublets are consistent with the HS Fe^{2+} and Fe^{3+} ions, which have similar local coordination geometries to magnesium in our silicate glass sample (Figs. 5 and 6) (Burns 1994; Dyar 1985; Dyar et al. 2006).

Previous experimental and theoretical studies on silicate perovskite have shown that Fe^{2+} exhibits a reduction in the QS going through the HS to LS transition, whereas the QS of Fe^{3+} would significantly increase to higher than 2 mm/s through the transition (Bengtson et al. 2009; Hsu et al. 2011, 2012; Lin et al. 2012; McCammon et al. 2010) (Fig. 5). However, we have observed a significant increase in the QS of Fe^{2+} between 4 and 55 GPa and reaching as high as 3.5 mm/s above 55 GPa (Fig. 2). Such high-QS values of Fe^{2+} have also been observed to occur in silicate perovskite, post-perovskite, garnet as well as silicate glasses at high pressures (Gu et al. 2012; Hsu et al. 2011, 2012; Lin et al. 2008, 2012; Mao et al. 2010; McCammon et al. 2008) (Fig. 5), with QS values as high as 4 mm/s in these phases. Although the QS of the Fe sites in Gu et al. (2012) follows a similar trend with pressure compared to our results (Fig. 5), they have used a three-doublet model to interpret their SMS spectra, in, which the ratio of the doublet abundances between Fe^{2+} and Fe^{3+} was allowed to vary with pressure. Since their SMS spectra were collected between 1 bar and 93 GPa at 300 K, oxidation states of iron ions were unlikely to vary in these glasses, unless a chemical reaction occurred (Gu et al. 2012; Potapkin et al. 2013) and introduced potential bias in the modeled results.

The high-QS values of Fe^{2+} observed in silicate perovskite and post-perovskite at high pressures have been explained as a result of the occurrence of the intermediate-spin state in earlier studies (Lin et al. 2008; McCammon et al. 2008; Mao et al. 2010), but most recent theoretical and experimental studies have sufficiently indicated that atomic site change and lattice distortion are likely the cause for the occurrence of the high QS (Hsu et al. 2011, 2012). The reduction in the derived S values in these experiments can now be explained as a result of the peak broadening effect that caused the satellite intensity to decrease (Figs. 3 and 4) (Lin et al. 2005). Indeed, iron-bearing pyrope has the highest QS among all known rock-forming minerals at ambient conditions

as a result of the strong lattice distortion in the garnet structure (Lyubutin and Dodokin 1970; Mao et al. 2013). The extremely high QS of Fe^{2+} in silicate glasses observed here could also be explained by the strong distortion of the local environment at high pressures, similar to the effect of Al in aluminosilicate glasses characterized by a pressure-induced increase in the quadrupolar coupling constant.

On the other hand, both theoretical calculations and experimental studies have reported significant changes in the coordination numbers of the Mg^{2+}, Si^{4+}, and Al^{3+} cations in silicate glasses at high pressures (Benmore et al. 2011; Lee et al. 2008; Stixrude and Karki 2005; Wilding et al. 2012). The increase in the averaged coordination number has been known to be associated with a marked increase in the density of the glass, known as glass densification (Stixrude and Karki 2005), and in the shear wave velocity (Murakami and Bass 2011). For example, the coordination number of Mg in a Mg_2SiO_4 glass is reported to increase from 5 at 1 bar to 6.6 at 30 GPa (Benmore et al. 2011). For the Fe-bearing silicate glasses, it has been reported that both Fe^{2+} and Fe^{3+} cations likely reside in a similar local coordination geometry as Mg^{2+} cation (Eckersley et al. 1988), and are expected to undergo significant changes in local atomic environments as well as densifications at high pressures. Furthermore, Fe^{3+} may act as a network former because of the high-Fe^{3+}/Fe ratio in our silicate glass samples (>0.5), leading to a denser structure in glass by decreasing the fraction of the non-bridging oxygen with pressure, similar to the behavior of Al^{3+} in aluminosilicates (Burkhard 2000; Lee 2010; Mysen and Richet 2005).

Quadrupole splitting and coordination number of iron in silicate glasses

To understand the relationship between the averaged coordination numbers of Fe ions and their associated QS values, we have summarized the QS values of minerals and glasses for different Fe valence states and local geometries at ambient conditions (Fig. 6) (Burns 1994; Dyar 1985; Dyar et al. 2006; Jackson et al. 2005; Rossano et al. 1999). In general, increasing the coordination number in minerals tends to elevate the value of QS for Fe^{2+} and/or Fe^{3+} (Fig. 6). The QS of Fe^{2+} increases from 1 mm/s in the fourfold-coordination environment to over 3 mm/s in eightfold coordination, although Fe^{2+} in minerals in the eightfold to twelvefold coordination, such as that in the A site of the silicate perovskite, has a QS value lower than that of the eightfold coordination (Fig. 6). Most of the silicate glasses exhibit a greater QS value for Fe^{2+} and/or Fe^{3+} in the sixfold coordination than in the fourfold coordination, yet a few exceptions with higher coordination numbers display a relatively small QS value (Dyar and Birnie 1984; Dyar and Burns 1981). Although experimental studies on the QS value of Fe in the fivefold coordination are limited, QS of Fe^{2+} in the five-coordination is similar to that in the six-coordination (Jackson et al. 2005; Rossano et al. 1999). The averaged coordination number of the Mg and Fe cations is reported to be approximately six in average in $MgSiO_3$ glasses (Funamori et al. 2004). Comparison of our high-pressure SMS results with these literature values indicate that the QS values of our glasses at high pressures are higher than those with a coordination number of six (Fig. 6). Iron ions in our (Al,Fe)-silicate glass would have an enhanced coordination number of

higher than six at high pressures (Lee 2010; Wilding et al. 2012) (Fig. 6). Based on these analyses, we thus conclude that the enhanced QS in the (Al,Fe)-silicate glass should be associated with enhanced density, coordination number, and distortion of the local environments of the (Mg,Fe) ions (Benmore et al. 2011; Wilding et al. 2012).

IMPLICATIONS AND CONCLUSIONS

Based on both XES and SMS analyses of our results and relevant literature data, we conclude that both Fe^{2+} and Fe^{3+} ions in the similar local atomic environment to magnesium in the Al-bearing silicate glass have relatively high-QS values in the HS state up to 126 GPa. The high-QS values are likely a result of the enhanced density, coordination number, and distortion of the local cation environments. Correcting the broadening effect in XES spectra as a function of pressure reveals no significant changes in the derived total spin number within experimental uncertainties, indicating that all iron ions remain in the HS state at high pressures. Here our results also show that iron ions in silicate glasses exhibit similar electronic states to mantle minerals at high pressures (Lin et al. 2013). Previous experimental study on silicate perovskite has shown that increasing temperature can increase the Fe^{3+}/(Fe^{2+}+Fe^{3+}) ratio through thermal activation, but does not affect the stability of the Fe spin states to pressure (Fei et al. 1994). This could be also true for our silicate glasses, although the effect of temperature on the spin and valence states of silicate glass remains to be further investigated. However, if some of the Fe^{3+} resides in a local environment similar to Si^{4+} in silicate glasses at high temperatures as a result of the thermal activation (Fei et al. 1994), Fe^{3+} ions may undergo the HS to LS transition at lower-mantle pressure-temperature conditions (Hsu et al. 2011; Tsuchiya and Wang 2013), leading to potential changes in density, incompressibility, and transport properties of silicate glasses (Lin et al. 2013). Since these silicate glasses are synthesized by cooling a supercooled liquid below the glass transition pressure that produces some similarities in local structures to melts, our results here may be used as analogs to understanding spin and valence states of iron in melts in the deep-Earth mantle (Akins et al. 2004; Henderson et al. 2006; McMillan 1984; Mysen and Richet 2005).

REFERENCES CITED

Akins, J.A., Luo, S.N., Asimow, P.D., and Ahrens, T.J. (2004) Shock-induced melting of MgSiO3 perovskite and implications for melts in Earth's lowermost mantle. Geophysical Research Letters, 31, L14612, DOI: 10.1029/2004gl020237.
Alberto, H.V., daCunha, J.L.P., Mysen, B.O., Gil, J.M., and deCampos, N.A. (1996) Analysis of Mössbauer spectra of silicate glasses using a two-dimensional Gaussian distribution of hyperfine parameters. Journal of Non-Crystalline Solids, 194, 48–57.
Andrault, D., Petitgirard, S., Lo Nigro, G., Devidal, J.L., Veronesi, G., Garbarino, G., and Mezouar, M. (2012) Solid-liquid iron partitioning in Earth's deep mantle. Nature, 487, 354–357.

Badro, J., Fiquet, G., Guyot, F., Rueff, J.P., Struzhkin, V.V., Vankó, G., and Monaco, G. (2003) Iron partitioning in Earth's mantle: Toward a deep lower mantle discontinuity. Science, 300, 789–791.

Bengtson, A., Li, J., and Morgan, D. (2009) Mössbauer modeling to interpret the spin state of iron in (Mg,Fe)SiO3 perovskite. Geophysical Research Letters, 36, L15301, DOI: 10.1029/2009gl038340.

Benmore, C.J., Soignard, E., Guthrie, M., Amin, S.A., Weber, J.K.R., McKiernan, K., Wilding, M.C., and Yarger, J.L. (2011) High pressure X-ray diffraction measurements on Mg2SiO4 glass. Journal of Non-Crystalline Solids, 357, 2632–2636.

Bonnin-Mosbah, M., Simionovici, A.S., Metrich, N., Duraud, J.P., Massare, D., and Dillmann, P. (2001) Iron oxidation states in silicate glass fragments and glass inclusions with a XANES micro-probe. Journal of Non-Crystalline Solids, 288, 103–113.

Boon, J.A., and Fyfe, W.S. (1972) Coordination number of ferrous ions in silicate-glasses. Chemical Geology, 10, 287–298.

Burkhard, D.J.M. (2000) Iron-bearing silicate glasses at ambient conditions. Journal of Non-Crystalline Solids, 275, 175–188.

Burns, R.G. (1994) Mineral mössbauer-spectroscopy—correlations between chemical-shift and quadrupole splitting parameters. Hyperfine Interactions, 91, 739–745.

Calas, G., and Petiau, J. (1983) Coordination of iron in oxide glasses through high-resolution K-edge spectra—information from the pre-edge. Solid State Communications, 48, 625–629.

Cameron, A.G.W., and Benz, W. (1991) The origin of the moon and the single impact hypothesis-IV. Icarus, 92, 204–216.

Catalli, K., Shim, S.H., Prakapenka, V.B., Zhao, J.Y., Sturhahn, W., Chow, P., Xiao, Y.M., Liu, H.Z., Cynn, H., and Evans, W.J. (2010) Spin state of ferric iron in MgSiO3 perovskite and its effect on elastic properties. Earth and Planetary Science Letters, 289, 68–75.

Catalli, K., Shim, S.H., Dera, P., Prakapenka, V.B., Zhao, J.Y., Sturhahn, W., Chow, P., Xiao, Y.M., Cynn, H., and Evans, W.J. (2011) Effects of the Fe3+ spin transition on the properties of aluminous perovskite—New insights for lower-mantle seismic heterogeneities. Earth and Planetary Science Letters, 310, 293–302.

Corgne, A., Liebske, C., Wood, B.J., Rubie, D.C., and Frost, D.J. (2005) Silicate perovskite-melt partitioning of trace elements and geochemical signature of a deep perovskitic reservoir. Geochimica et Cosmochimica Acta, 69, 485–496.

de Groot, F. (2001) High resolution X-ray emission and X-ray absorption spectroscopy. Chemical Reviews, 101, 1779–1808.

Dyar, M.D. (1985) A review of Mössbauer data on inorganic glasses; the effects of composition on iron valency and coordination. American Mineralogist, 70, 304–316.

Dyar, M.D., and Birnie, D.P. (1984) Quench media effects on iron partitioning and ordering in a lunar glass. Journal of Non-Crystalline Solids, 67, 397–412.

Dyar, M.D., and Burns, R.G. (1981) Coordination chemistry of iron in glasses contributing to remote-sensed spectra of the moon. Proceedings of the Lunar and Planetary Science Conference, 12B, 695–702.

Dyar, M.D., Agresti, D.G., Schaefer, M.W., Grant, C.A., and Sklute, E.C. (2006) Mössbauer spectroscopy of earth and planetary materials. Annual Review of Earth and Planetary Sciences, 34, 83–125.

Eckersley, M.C., Gaskell, P.H., Barnes, A.C., and Chieux, P. (1988) Structural ordering in a calcium silicate glass. Nature, 335, 525–527.

Ediger, M.D., Angell, C.A., and Nagel, S.R. (1996) Supercooled liquids and glasses. Journal of Physical Chemistry, 100, 13200–13212.

Fei, Y., Virgo, D., Mysen, B.O., Wang, Y., and Mao, H.K. (1994) Temperature-dependent electron delocalization in (Mg,Fe)SiO3 perovskite. American Mineralogist, 79, 826–837.

Fox, K.E., Furukawa, T., and White, W.B. (1982) Transition-metal ions in silicate melts. Part 2. Iron in sodium-silicate glasses. Physics and Chemistry of Glasses, 23, 169–178.

Funamori, N., and Sato, T. (2010) Density contrast between silicate melts and crystals in the deep mantle: An integrated view based on static-compression data. Earth and Planetary Science Letters, 295, 435–440.

Funamori, N., Yamamoto, S., Yagi, T., and Kikegawa, T. (2004) Exploratory studies of silicate melt structure at high pressures and temperatures by in situ X-ray diffraction. Journal of Geophysical Research-Solid Earth, 109, B03203, DOI: 10.1029/2003jb002650.

Gavriliuk, A.G., Lin, J.F., Lyubutin, I.S., and Struzhkin, V.V. (2006) Optimization of the conditions of synchrotron Mössbauer experiment for studying electronic transitions at high pressures by the example of (Mg, Fe)O magnesiowustite. Journal of Experimental and Theoretical Physical Letters, 84, 161–166.

Giuli, G., Pratesi, G., Cipriani, C., and Paris, E. (2002) Iron local structure in tektites and impact glasses by extended X-ray absorption fine structure and high-resolution X-ray absorption near-edge structure spectroscopy. Geochimica et Cosmochimica Acta, 66, 4347–4353.

Giuli, G., Paris, E., Hess, K.U., Dingwell, D.B., Cicconi, M.R., Eeckhout, S.G., Fehr, K.T., and Valenti, P. (2011) XAS determination of the Fe local environment and oxidation state in phonolite glasses. American Mineralogist, 96, 631–636.

Goldman, D.S., and Berg, J.I. (1980) Spectral study of ferrous iron in Ca-Al-borosilicate glass at room and melt temperatures. Journal of Non-Crystalline Solids, 38–39, 183–188, DOI: 10.1016/0022-3093(80)90415-9.

Gu, C., Catalli, K., Grocholski, B., Gao, L.L., Alp, E., Chow, P., Xiao, Y.M., Cynn, H., Evans, W.J., and Shim, S.H. (2012) Electronic structure of iron in magnesium silicate glasses at high pressure. Geophysical Research Letters, 39, L24304, DOI: 10.1029/2012gl053950.

Guillot, B., and Sator, N. (2007) A computer simulation study of natural silicate melts. Part II: High pressure properties. Geochimica et Cosmochimica Acta, 71, 4538–4556.

Henderson, G.S., Calas, G., and Stebbins, J.F. (2006) The structure of silicate glasses and melts. Elements, 2, 269–273.

Hsu, H., Blaha, P., Cococcioni, M., and Wentzcovitch, R.M. (2011) Spin-state crossover and hyperfine interactions of ferric iron in MgSiO3 perovskite. Physical Review Letters, 106, 118501, DOI: 10.1103/Physrevlett.106.118501.

Hsu, H., Yu, Y.G., and Wentzcovitch, R.M. (2012) Spin crossover of iron in aluminous MgSiO3 perovskite and post-perovskite. Earth and Planetary Science Letters, 359–360, 34–39.

Jackson, W.E., Farges, F., Yeager, M., Mabrouk, P.A., Rossano, S., Waychunas, G.A., Solomon, E.I., and Brown, G.E. (2005) Multi-spectroscopic study of Fe(II) in silicate glasses: Implications for the coordination environment of Fe(II) in silicate melts. Geochimica et Cosmochimica Acta, 69, 4315–4332.

Lee, S.K. (2005) Microscopic origins of macroscopic properties of silicate melts and glasses at ambient and high pressure: Implications for melt generation and dynamics. Geochimica et Cosmochimica Acta, 69, 3695–3710.

——— (2010) Effect of pressure on structure of oxide glasses at high pressure: Insights from solid-state NMR of quadrupolar nuclides. Solid State Nuclear Magnetic Resonance, 38, 45–57.

——— (2011) Simplicity in melt densification in multicomponent magmatic reservoirs in Earth's interior revealed by multinuclear magnetic resonance. Proceedings of the National Academy of Sciences, 108, 6847–6852.

Lee, S.K., Lin, J.F., Cai, Y.Q., Hiraoka, N., Eng, P.J., Okuchi, T., Mao, H.K., Meng, Y., Hu, M.Y., Chow, P., and others. (2008) X-ray Raman scattering study of MgSiO3 glass at high pressure: Implication for triclustered MgSiO3 melt in Earth's mantle. Proceedings of the National Academy of Sciences, 105, 7925–7929.

Levy, R.A., Lupis, C.H.P., and Flinn, P.A. (1976) Mössbauer analysis of valence and coordination of iron cations in SiO2-Na2O-CaO glasses. Physics and Chemistry of Glasses, 17, 94–103.

Lin, J.F., Struzhkin, V.V., Mao, H.K., Hemley, R.J., Chow, P., Hu, M.Y., and Li, J. (2004) Magnetic transition in compressed Fe3C from X-ray emission spectroscopy. Physical Review B, 70, 212405, DOI: 10.1103/Physrevb.70.212405.

Lin, J.F., Struzhkin, V.V., Jacobsen, S.D., Hu, M.Y., Chow, P., Kung, J., Liu, H., Mao, H-K., and Hemley, R.J. (2005) Spin transition of iron in magnesiowüstite in the Earth's lower mantle. Nature, 436, 377–380.

Lin, J.F., Gavriliuk, A.G., Struzhkin, V.V., Jacobsen, S.D., Sturhahn, W., Hu, M.Y., Chow, P., and Yoo, C.S. (2006) Pressure-induced electronic spin transition of iron in magnesiowustite-(Mg,Fe)O. Physical Review B, 73, 113107, DOI: 10.1103/Physrevb.73.113107.

Lin, J.F., Watson, H., Vankó, G., Alp, E.E., Prakapenka, V.B., Dera, P., Struzhkin, V.V., Kubo, A., Zhao, J.Y., McCammon, C., and Evans, W.J. (2008) Intermediate-spin ferrous iron in lowermost mantle post-perovskite and perovskite. Nature Geoscience, 1, 688–691.

Lin, J.F., Mao, Z., Jarrige, I., Xiao, Y.M., Chow, P., Okuchi, T., Hiraoka, N., and Jacobsen, S.D. (2010) Resonant X-ray emission study of the lower-mantle ferropericlase at high pressures. American Mineralogist, 95, 1125–1131.

Lin, J.F., Alp, E.E., Mao, Z., Inoue, T., McCammon, C., Xia, Y.M., Chow, P., and Zhao, J.Y. (2012) Electronic spin states of ferric and ferrous iron in the lower-mantle silicate perovskite. American Mineralogist, 97, 592–597.

Lin, J.F., Speziale, S., Mao, Z., and Marquardt, H. (2013) Effects of the electronic spin transitions of iron in lower-mantle minerals: implications to deep-mantle geophysics and geochemistry. Review in Geophysics, 51, DOI: 10.1002/rog.20010.

Lyubutin, I.S., and Dodokin, A.P. (1970) Temperature dependence of the Mössbauer effect for Fe2+ in dodecahedral coordination in garnet. Kristallografiya, 15, 1249–1250.

Mao, H.K., Xu, J., and Bell, P.M. (1986) Calibration of the ruby pressure gauge to 800-Kbar under quasi-hydrostatic conditions. Journal of Geophysical Research-Solid Earth and Planets, 91, 4673–4676.

Mao, Z., Lin, J.F., Jacobs, C., Watson, H.C., Xiao, Y., Chow, P., Alp, E.E., and Prakapenka, V.B. (2010) Electronic spin and valence states of Fe in CaIrO3-type silicate post-perovskite in the Earth's lowermost mantle. Geophysical Research Letters, 37, L22304, DOI: 10.1029/2010gl045021.

Mao, Z., Lin, J.F., Scott, H.P., Watson, H.C., Prakapenka, V.B., Xiao, Y., Chow, P., and McCammon, C. (2011) Iron-rich perovskite in the Earth's lower mantle. Earth and Planetary Science Letters, 309, 179–184.

Mao, Z., Lin, J.F., Huang, S., Chen, J., Xiao, Y., and Chow, P. (2013) Synchrotron Mössbauer study of Fe-bearing pyrope at high pressures and temperatures. American Mineralogist, 98, 1146–1152.

McCammon, C., Kantor, I., Narygina, O., Rouquette, J., Ponkratz, U., Sergueev, I., Mezouar, M., Prakapenka, V., and Dubrovinsky, L. (2008) Stable intermediate-

spin ferrous iron in lower-mantle perovskite. Nature Geoscience, 1, 684–687.

McCammon, C., Dubrovinsky, L., Narygina, O., Kantor, I., Wu, X., Glazyrin, K., Sergueev, I., and Chumakov, A.I. (2010) Low-spin Fe^{2+} in silicate perovskite and a possible layer at the base of the lower mantle. Physics of the Earth and Planetary Interiors, 180, 215–221.

McMillan, P. (1984) Structural studies of silicate-glasses and melts; applications and limitations of Raman-spectroscopy. American Mineralogist, 69, 622–644.

Murakami, M., and Bass, J.D. (2011) Evidence of denser $MgSiO_3$ glass above 133 gigapascal (GPa) and implications for remnants of ultradense silicate melt from a deep magma ocean. Proceedings of the National Academy of Sciences, 108, 17286–17289.

Mysen, B., and Richet, P. (2005) Silicate Glasses and Melts. Elsevier Science.

Mysen, B.O., and Virgo, D. (1989) Redox equilibria, structure, and properties of Fe-bearing aluminosilicate melts—Relationships among temperature, composition, and oxygen fugacity in the system $Na_2O-Al_2O_3-SiO_2-Fe-O$. American Mineralogist, 74, 58–76.

Mysen, B.O., Virgo, D., and Seifert, F.A. (1984) Redox equilibria of iron in Alkaline-Earth silicate melts—relationships between melt structure, oxygen fugacity, temperature and properties of iron-bearing silicate liquids. American Mineralogist, 69, 834–847.

Mysen, B.O., Virgo, D., Neumann, E.R., and Seifert, F.A. (1985) Redox equilibria and the structural states of ferric and ferrous iron in melts in the system $CaO-MgO-Al_2O_3-SiO_2-Fe-O$—Relationships between redox equilibria, melt structure and liquidus phase-equilibria. American Mineralogist, 70, 317–331.

Nolet, D.A. (1980) Optical-absorption and Mössbauer-spectra of Fe, Ti silicate-glasses. Journal of Non-Crystalline Solids, 37, 99–110.

Nomura, R., Ozawa, H., Tateno, S., Hirose, K., Hernlund, J., Muto, S., Ishii, H., and Hiraoka, N. (2011) Spin crossover and iron-rich silicate melt in the Earth's deep mantle. Nature, 473, 199–202.

Ohtani, E. (1985) The primordial terrestrial magma ocean and its implication for stratification of the mantle. Physics of the Earth and Planetary Interiors, 38, 70–80, DOI: 10.1016/0031-9201(85)90123-2.

Poe, B.T., McMillan, P.F., Rubie, D.C., Chakraborty, S., Yarger, J., and Diefenbacher, J. (1997) Silicon and oxygen self-diffusivities in silicate liquids measured to 15 gigapascals and 2800 kelvin. Science, 276, 1245–1248.

Potapkin, V., McCammon, C., Glazyrin, K., Kantor, A., Kupenko, I., Prescher, C., Sinmyo, R., Smirnov, G.V., Chumakov, A.I., Ruffer, R., and Dubrovinsky, L. (2013) Effect of iron oxidation state on the electrical conductivity of the Earth's lower mantle. Nature Communications, 4, 1427, DOI: 10.1038/Ncomms2436.

Rigden, S.M., Ahrens, T.J., and Stolper, E.M. (1984) Densities of liquid silicates at high-pressures. Science, 226, 1071–1074.

Rossano, S., Balan, E., Morin, G., Bauer, J.P., Calas, G., and Brouder, C. (1999) ^{57}Fe Mössbauer spectroscopy of tektites. Physics and Chemistry of Minerals, 26, 530–538.

Rossano, S., Ramos, A., Delaye, J.M., Creux, S., Filipponi, A., Brouder, C., and Calas, G. (2000) EXAFS and molecular dynamics combined study of $CaO-FeO-2SiO_2$ glass. New insight into site significance in silicate glasses. Europhysics Letters, 49, 597–602.

Rueff, J.P., Shukla, A., Kaprolat, A., Krisch, M., Lorenzen, M., Sette, F., and Verbeni, R. (2001) Magnetism of Invar alloys under pressure examined by inelastic X-ray scattering. Physical Review B, 63, 132409, DOI: 10.1103/Physrevb.63.132409.

Rueff, J.P., Krisch, M., and Lorenzen, M. (2002) Magnetic transitions in Fe_3Pt Invar alloy under high pressure and temperature studied by inelastic X-ray scattering. High Pressure Research, 22, 53–56.

Stevenson, D.J. (1987) Origin of the moon—the collision hypothesis. Annual Review of Earth and Planetary Sciences, 15, 271–315.

Stixrude, L., and Karki, B. (2005) Structure and freezing of $MgSiO_3$ liquid in Earth's lower mantle. Science, 310, 297–299.

Stolper, E., Walker, D., Hager, B.H., and Hays, J.F. (1981) Melt segregation from partially molten source regions—The importance of melt density and source region size. Journal of Geophysical Research, 86, 6261–6271.

Sturhahn, W. (2000) CONUSS and PHOENIX: Evaluation of nuclear resonant scattering data. Hyperfine Interactions, 125, 149–172.

Tonks, W.B., and Melosh, H.J. (1993) Magma Ocean Formation Due to Giant Impacts. Journal of Geophysical Research-Planets, 98, 5319–5333, DOI: 10.1029/92je02726.

Tsuchiya, T., and Wang, X. (2013) Ab initio investigation on the high-temperature thermodynamic properties of Fe^{3+}-bearing $MgSiO_3$ perovskite. Journal of Geophysical Research, 118, 83–91.

Vankó, G., Neisius, T., Molnar, G., Renz, F., Karpati, S., Shukla, A., and de Groot, F.M.F. (2006) Probing the 3d spin momentum with X-ray emission spectroscopy: The case of molecular-spin transitions. Journal of Physical Chemistry B, 110, 11647–11653.

Virgo, D., and Mysen, B.O. (1985) The structural state of iron in oxidized vs. reduced glasses at 1 atm—A ^{57}Fe Mössbauer study. Physics and Chemistry of Minerals, 12, 65–76.

Wang, Z.F., Cooney, T.F., and Sharma, S.K. (1995) In-situ structural investigation of iron-containing silicate liquids and glasses. Geochimica et Cosmochimica Acta, 59, 1571–1577.

Waychunas, G.A., Brown, G.E., Ponader, C.W., and Jackson, W.E. (1988) Evidence from X-ray absorption for network-forming Fe^{2+} in molten alkali silicates. Nature, 332, 251–253.

Wen, L.X., and Helmberger, D.V. (1998) Ultra-low velocity zones near the core-mantle boundary from broadband PKP precursors. Science, 279, 1701–1703.

Wilding, M., Guthrie, M., Kohara, S., Bull, C.L., Akola, J., and Tucker, M.G. (2012) The structure of $MgO-SiO_2$ glasses at elevated pressure. Journal of Physics-Condensed Matter, 24, 339501, DOI: 10.1088/0953-8984/24/33/339501.

Wilke, M., Farges, F., Petit, P.E., Brown, G.E., and Martin, F. (2001) Oxidation state and coordination of Fe in minerals: An Fe K-XANES spectroscopic study. American Mineralogist, 86, 714–730.

Wilke, M., Schmidt, C., Farges, F., Malavergne, V., Gautron, L., Simionovici, A., Hahn, M., and Petit, P.E. (2006) Structural environment of iron in hydrous aluminosilicate glass and melt-evidence from X-ray absorption spectroscopy. Chemical Geology, 229, 144–161.

Williams, Q., and Garnero, E.J. (1996) Seismic evidence for partial melt at the base of Earth's mantle. Science, 273, 1528–1530.

Wolf, G.H., and McMillan, P.F. (1995) Pressure effects on silicate melt—Structure and properties. In J.F. Stebbins, F. McMillan, and D.B. Dingwell, Eds. Structure, Dynamics, and Properties of Silicate Melts, 32, p. 505–562. Reviews in Mineralogy, Mineralogical Society of America, Chantilly, Virginia.

Yarger, J.L., Smith, K.H., Nieman, R.A., Diefenbacher, J., Wolf, G.H., Poe, B.T., and McMillan, P.F. (1995) Al coordination changes in high-pressure aluminosilicate liquids. Science, 270, 1964–1967.